Wideband Temporal Spectrum Sensing Using Cepstral Features

Hanke Cheng, Brian L. Mark, and Yariv Ephraim
Dept. of Electrical and Computer Eng.
George Mason University
4400 University Drive, MS 1G5
Fairfax, VA 22030
email: { hcheng7, bmark, yephraim }@gmu.edu

***Abstract*—Spectrum sensing enables secondary users in a cognitive radio network to opportunistically access portions of the spectrum left idle by primary users. Tracking spectrum holes jointly in time and frequency over a wide spectrum band is a challenging task. In one approach to wideband temporal sensing, the spectrum band is partitioned into narrowband subchannels of fixed bandwidth, which are then characterized via hidden Markov modeling using average power or energy measurements as observation data. Adjacent, correlated subchannels are recursively aggregated into channels of variable bandwidths, corresponding to the primary user signals. Thus, wideband temporal sensing is transformed into a multiband sensing scenario by identifying the primary user channels in the spectrum band. However, future changes in the configuration of the primary user channels in the multiband setup cannot generally be detected using an energy detector front end for spectrum sensing. We propose the use of a cepstral feature vector to detect changes in the spectrum envelope of a primary user channel. Our numerical results show that the cepstrum-based spectrum envelope detector performs well under moderate to high signal-to-noise ratio conditions.**[1]

***Index Terms*—Cognitive radio; dynamic spectrum access; spectrum sensing; cepstrum; hidden Markov model.**

I. Introduction

Due to the rapidly increasing number of wireless systems and devices, the demand for wireless spectrum resources has been increasing at a remarkable rate over the past two decades. As a result, the crowded radio spectrum under 5 GHz has become a bottleneck for wireless communications. To address the spectrum scarcity problem, cognitive radio technologies are a promising direction of research for achieving more efficient utilization of the spectrum. In practice, large portions of the spectrum under 5 GHz remain highly underutilized due to intermittent spectrum usage by licensed users across the dimensions of frequency, space, and time. This observation has been verified experimentally, for example, in the spectrum occupancy measurement report published by Federal Communications Commission (FCC) in 2002 [1] and more recently in spectrum studies conducted by the Shared Spectrum Company [2]. Such studies point to potentially significant gains in spectrum utilization that could be achieved via cognitive radio technologies.

In this paper, we focus on wideband temporal spectrum sensing, i.e., tracking spectrum holes jointly in time and frequency across a wide spectrum band. For concreteness, we adopt the hierarchical access model of dynamic spectrum access, which consists of licensed or primary users (PUs) and unlicensed or secondary users (SUs) [3]. The SUs perform spectrum sensing to detect and exploit the spectrum left idle by the PUs without causing harmful interference to the PUs. In this scenario, reliable spectrum sensing is the prerequisite of dynamic spectrum access in cognitive radio network. Other dynamic spectrum sharing paradigms also require an effective means for detecting and exploiting spectrum holes.

Various spectrum sensing approaches have been developed such as energy detection, matched filter detection, and cyclostationary feature detection [4]. The energy detector simply computes the average power of the received signal over a block of received signal samples and compares it to a specific threshold. This detector has the lowest computational complexity but performs poorly under low signal-to-noise ratio (SNR). The matched filter detector requires prior knowledge about the transmitted signal and thus its applicability is limited. The cyclostationary feature detector utilizes the cyclostationary property of digital modulated signals and makes decisions by computing certain test statistics from the cyclic spectrum of the received signal. The performance of the cyclostationary feature detector is generally superior compared to the energy detector, especially under low SNR, but it requires a much larger number of received signal samples and has significantly higher computational complexity. The aforementioned spectrum sensing approaches provide a snapshot of spectrum occupancy in the frequency domain, but do not detect temporal spectrum holes.

Spectrum detectors based on an underlying hidden Markov model with an energy detector front end have been developed for offline and online temporal spectrum sensing of *narrowband* channels [5], [6]. A generalization of the HMM, referred to as a hidden bivariate Markov model (HBMM) was proposed in [5] to account for more general sojourn time distributions of a given PU in the idle and active states. In the

[1]This work was supported in part by the U.S. National Science Foundation under Grants No. 1421869 and 1737989.

temporal spectrum sensing approach of [5], an HBMM model is first trained offline via an observation sequence consisting of average received signal powers. The Baum algorithm is used to estimate the parameter of the trained HBMM model. Spectrum sensing is accomplished by using average received power measurements as observations to compute the posterior probability of the underlying state of the PU given the observation sequence, based on the trained HBMM. An online approach to estimating the HBMM model parameter in this context is developed in [6]. The performance of the HBMM-based detector is better than that of an energy detector alone and enables prediction of future spectrum occupancy.

The present paper builds upon the wideband temporal sensing approach proposed in [7] whereby a given frequency band is first partitioned into narrowband channels of smaller but equal bandwidth. The narrowband channels are then sensed individually using an HMM-based approach similar to that of [5]. Adjacent channels that are determined to be correlated according to a modified correlation metric are aggregated to form larger channels. The procedure is conducted in a recursive manner, which ultimately results in the identification of a set of PU channels together with associated HMM parameters. Temporal spectrum sensing can then be applied to the identified PU channels in a multiband spectrum sensing setup. However, the recursive wideband temporal sensing approach in [7] is performed offline and does not adapt to dynamic changes in the PU channels that may occur at a later time. For example, a PU channel may at some future time be occupied by more than two PU signals. In this case, the multiband sensing configuration should be recomputed. The energy detector front end used in [5]–[7] cannot be used effectively to detect a change in the spectrum envelope of a PU channel.

In this paper, we develop an approach to wideband temporal spectrum sensing that can adapt to dynamic changes in the configuration of a PU channel. A key component of our approach is the use of a cepstral feature vector to detect changes in the spectrum envelope of a PU signal within a given frequency band. The cepstral vector at a given time frame characterizes the spectrum envelope of a PU signal. Our approach extends that of [7] for determining an initial multiband configuration of PU channels by providing a method to determine when the multiband setup should be recomputed. To illustrate the problem, Fig. 1 shows three scenarios with respect to a given spectrum band. Figures 1(a) and 1(b) depict the spectrum occupancy when the band is, respectively, idle and active. In Fig. 1(c), apparently the two halves of the band can be seen to be in different states. In this case, the band cannot be characterized as a single PU channel. By using the cepstrum, a spectrum envelope change within a designated PU channel can be detected efficiently.

The remainder of the paper is organized as follows. In Section II, we describe a framework for wideband temporal spectrum sensing, which involves the proposed method for detecting spectrum envelope changes. In Section III, we develop the cepstrum-based spectrum envelope detector. We present numerical results in Section IV. The paper is concluded in Section V.

II. Spectrum Sensing Framework

In this section, we describe a framework for wideband temporal spectrum sensing based on the narrowband temporal sensing approach in [5] and the recursive algorithm for aggregating narrowband subchannels into PU channels in [7].

A. Narrowband Temporal Sensing

We adopt the narrowband sensing approach in [5] based on hidden Markov modeling of a given channel and application of the Baum algorithm to estimate its parameter. Consider the scenario of a PU transmitting on a narrowband channel while an SU extracts measurements of the received signal on this channel. As in [8], the channel state of the PU is a discrete-time process $X = \{X_t : t = 0, 1, \ldots\}$ where

$$X_t = \begin{cases} 0, & \text{idle state,} \\ 1, & \text{active state} \end{cases} \tag{1}$$

at time t. The observation data obtained by the SU consists of a discrete-time process $\boldsymbol{Y} = \{\boldsymbol{Y}_t\}$, where $\boldsymbol{Y}_t$ denotes a vector of observations and is represented by a multivariate Gaussian random variable with mean $\boldsymbol{\mu}_a$ and covariance matrix $\boldsymbol{\Sigma}_a$, given the channel state of the PU, i.e., $X_t = a$, where $a \in \{0, 1\}$. In [5], the observation data at time t was a scalar Y_t, representing the average power or energy of the received signal at time t. In the present paper, the observation data is a feature vector $\boldsymbol{Y}_t$ derived from the cepstrum of the received signal (see Section III). The observation vectors in the sequence $\{\boldsymbol{Y}_t\}$ are assumed statistically independent. The mean and covariance matrix of each $\boldsymbol{Y}_t$ depends on the state X_t, i.e., $\boldsymbol{Y}$ is conditionally Gaussian given X. In the approach of [5], average received power measurements on a narrowband PU channel form the observation sequence Y. When the underlying state process X is a discrete-time Markov chain, the bivariate process (Y, X) is a hidden Markov model. Given an estimate of the parameter of the HMM and the sequence of observations up to the current time t, the current state and future states of X can be estimated.

An HMM may not be sufficient to accurately model the channel state process for temporal spectrum sensing, since the sojourn time of the process X in a given state is limited to having a geometric distribution. To address this issue, the hidden bivariate Markov model was proposed in [5] to extend the chain X to a bivariate Markov chain $Z = (X, S)$ with an auxiliary process S such that the process X alone is not a Markov chain. Thus, the HBMM is a trivariate process (Y, X, S). Instead of the geometric distribution, the sojourn times of the X-state have a discrete phase-type distribution, which can approximate a large class of discrete-time sojourn time distributions including mixtures and convolutions of geometric distributions. For a general HBMM, the state space of X is denoted by $\mathbb{X} = \{0, 1, \ldots, d-1\}$ where d is a positive integer, and that of S is denoted by $\mathbb{S} = \{1, 2, \ldots, r\}$ where r is positive integer. In this paper, $d = 1$ such that $\mathbb{X} = \{0, 1\}$.

The state space of Z is given by $\mathbb{Z} = \mathbb{X} \times \mathbb{S}$. When $r = 1$, the HBMM reduces to an HMM.

Let $\phi = \{\boldsymbol{\pi}, \boldsymbol{G}, \boldsymbol{\mu}_a, \boldsymbol{\Sigma}_a\}$ denote the parameter of the HBMM used to model a given channel. The vector $\boldsymbol{\pi} = [\pi_{a,i} : (a,i) \in \mathbb{Z}]$, of size dr, represents the initial distribution of each state Z, where $\pi_{a,i} = P(Z_0 = (a,i))$. The transition matrix $\boldsymbol{G}$ of the HBMM is a $dr \times dr$ matrix consisting of the probabilities $g_{ab}(ij) = P(Z_t = (b,j) \mid Z_{t-1} = (a,i))$ of transition from state (a,i) to (b,j). The other two components of the HBMM parameter, $\boldsymbol{\mu}_a$ and $\boldsymbol{\Sigma}_a$, are the mean vector and the covariance matrix of the Gaussian distribution given channel state $X = a$, respectively. As discussed in [5], the Baum algorithm can be applied to estimate the parameter of an HBMM for temporal spectrum sensing of a narrowband sensing. Given an observation sequence $\boldsymbol{y}_0^T = \{\boldsymbol{y}_0, \boldsymbol{y}_1, \ldots, \boldsymbol{y}_T\}$, each iteration of the Baum algorithm computes a new parameter estimate $\hat{\phi}$ based on the previous estimate ϕ. The re-estimation formulas given a scalar observation sequence y_0^T of average power measurements $\{y_t\}$ are given in [5, Eq. (18)-(21)] and generalize straightforwardly to the case of vector observations considered here.

B. Wideband Temporal Sensing

In the wideband temporal sensing approach of [7], a given spectrum band is partitioned hierarchically into narrowband channels, each of which is characterized by an HMM or, more generally an HBMM, as discussed above. A recursive tree search is used to aggregate adjacent, statistically correlated narrowband channels into PU channels of generally larger bandwidth. Thus, the original spectrum band is divided into a set of PU channels, each of which is then monitored for temporal spectrum hole opportunities via the hidden Markov modeling approach of [5]. In effect, the problem of sensing a given wide spectrum band jointly in time and frequency is transformed into a multiband spectrum sensing problem. In the multiband setup, each PU channel can be sensed independently using narrowband temporal sensing techniques. A challenge in multiband sensing is how to allocate computational resources in sensing a given set of PU channel to achieve a good tradeoff between computational effort and the amount of idle spectrum that can be detected [9].

An important issue not addressed in [7] is that the configuration of PU signal within the given spectrum band may change over time, i.e., the PU channels in the multiband setup may not be static. For example, a given PU channel determined through the approach of [7] alternates between an idle state, as in Fig. 1(a), and an active state, as in Fig. 1(b). After some time, the same channel may come to occupied by two PU signals that are active and idle at different times, as shown in Fig. 1(c). In this scenario, narrowband sensing can no longer be applied meaningfully to the channel. If such a change in the configuration of the PU channel can be detected, a new configuration can be recomputed using the approach of [7]. The key challenge here is to devise an efficient method to detect a change in the configuration of a given PU channel. This cannot be done using only the average power of the PU channel, since a change in the configuration of the PU channel may not involve a change in its average power. This motivates the cepstrum-based spectrum envelope detector proposed in the next section.

III. Cepstrum-based Spectrum Envelope Detector

We propose to augment the energy detector front end used for narrowband temporal spectrum sensing with a detector that uses cepstral features to determine changes in the spectrum envelope of a PU channel.

A. Cepstrum

Cepstral analysis has been widely used in applications such as mechanical inspection [10], seismic echo characterization [11], and automatic speech recognition [12]. The cepstrum of a signal is defined as the inverse Fourier transform of the logarithm of its power spectral density. Consider a signal $w(n)$ with power spectral density $S_w(k)$. The cepstral coefficients are given by

$$C_w(n) = \frac{1}{K} \sum_{k=0}^{K-1} \log(S_w(k)) \exp\left(j \frac{2\pi}{K} kn\right), \qquad (2)$$

where $\log(\cdot)$ denotes the natural logarithm and K is the frame of the signal. Estimates of the cepstral coefficients are derived from the periodogram estimate of the power spectral density, given as follows:

$$\hat{S}_w(k) = \frac{1}{N} |W(k)|^2. \qquad (3)$$

Here, $W(k)$ is the Discrete Fourier Transform (DFT) of $w(n)$:

$$W(k) = \sum_{n=0}^{N-1} w(n) \exp\left(-j \frac{2\pi}{K} kn\right), \qquad (4)$$

where $k = 0, \ldots, K-1$ and N is the number of samples of $w(n)$ used. Then the estimates for the cepstral coefficients are given by

$$c_w(n) = \frac{1}{K} \sum_{k=0}^{K-1} \log\left(\frac{1}{N} |W(k)|^2\right) \exp\left(j \frac{2\pi}{K} kn\right), \qquad (5)$$

for $n = 0, \ldots, K-1$. We assume $K \geq 2N - 1$ which makes $\hat{S}_w(k)$ the DFT of a linear sample correlation of $\{w(n)\}_{n=0}^{N-1}$ rather than a circular sample correlation.

The cepstral feature vector used for spectrum envelope change detection is formed from the first few cepstral coefficients as follows:

$$\boldsymbol{c}_w := (c_w(1), \ldots, c_w(L-1)), \qquad (6)$$

where $L \ll N$. The zeroth component $c_w(0)$ is closely related to the energy of the signal and may be used in lieu of the average signal power for temporal spectrum sensing based on the HBMM. However, this component is omitted in the cepstral feature vector given by (6), as it is not helpful for detecting a change in the configuration of a PU channel. The cepstrum, including the zeroth component, characterizes the envelope of the logarithm of the power spectral density of the

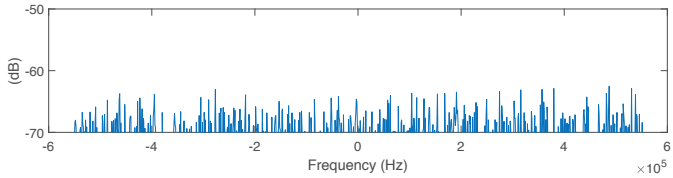

(a) Entire band is idle

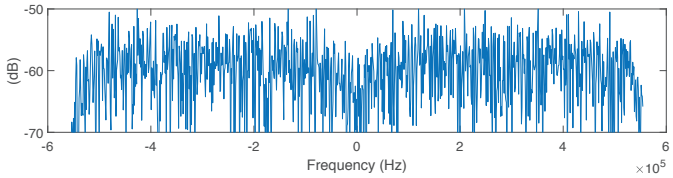

(b) Entire band is occupied

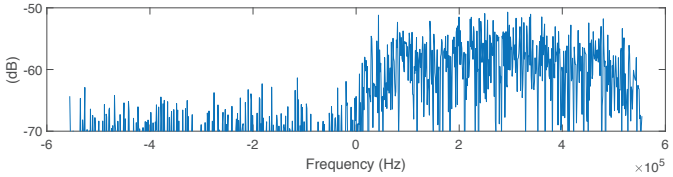

(c) Part of the band is occupied

Fig. 1: Spectrum envelope of a band in three scenarios.

signal. A typical length of the cepstral coefficient vector for speech recognition is $L = 12$ [12]. It was shown in [12] that the covariance of the cepstral components is approximately constant independent of the underlying signal:

$$\mathrm{cov}(c_w(n), c_w(m)) \approx \begin{cases} \frac{\pi^2}{3K}, & \text{if } n = m = 0, \frac{K}{2}, \\ \frac{\pi^2}{6K}, & \text{if } 0 < n = m < \frac{K}{2}, \\ 0. & \text{otherwise.} \end{cases} \tag{7}$$

for large K. This avoids the need to estimate the covariance matrix of the cepstral feature vector.

B. Spectrum Envelope Detector

Assume that a number of samples are collected in a given time period over a specific band. This period consists of two phases. Initially, we use the wideband temporal spectrum sensing approach in [7] to identify and characterize all of the subbands occupied by PU signals. Each subband is treated as an independent PU channel, characterized by an HBMM parameter estimate, and is initially said to be in *phase 1*. Spectrum sensing of the PU channels proceeds in a multiband setup using the HBMM parameter estimate and average power measurements. At the same time, a spectrum envelope detector based on the cepstral feature vector (6) is applied to detect a transition of the PU channel to a different configuration, which we refer to as *phase 2*. In phase 2, the channel no longer corresponds to a single PU signal. For example, Fig. 1(c) shows the spectrum envelope of a subband that is in *phase 2* because it consists of two parts that occupy the spectrum differently. Since the transition from phase 1 to phase 2 leads to a spectrum envelope change, we use the cepstral feature vector to detect it. After detecting the transition, the configuration of the PU channels in the orignal band of interest will need to be recomputed. This could be done by re-applying the approach of [7] to a portion of the original spectrum band containing the PU channel in phase 2.

The spectrum envelope detector is based on the underlying HBMM as discussed in Section II-A in which the observation vector $\boldsymbol{y}_t$ corresponds to the cepstral feature vector extracted from the received signal. The posterior probability that the channel is in the idle state given the sequence of observations $\boldsymbol{y}_0^t$ is denoted by $P(X_t = 0 \mid \boldsymbol{y}_0^t; \phi)$, where ϕ denotes the current estimate of the HBMM parameter for the channel. This probability can be derived from the scaled forward recursion of the Baum algorithm applied to the HBMM $(\boldsymbol{Y}, X, S)$. A *sample* decision $\hat{D}_t$ on whether a spectrum envelope change, i.e., a transition to phase 2, has occurred at time t is computed as follows:

$$\hat{D}_t = \begin{cases} 1, & \text{if } \gamma < P(X_t = 0 \mid \boldsymbol{y}_0^t; \phi) < 1 - \gamma, \\ 0, & \text{otherwise.} \end{cases} \tag{8}$$

where $\gamma \in (0, 0.5)$ is a constant. When $\hat{D}_t = 1$, a spectrum envelope change is detected, the rationale being that the posterior probability of the channel state is bounded away from the values 0 and 1 by γ. The choice of γ affects the probabilities of false alarm and detection of the spectrum envelope detector. If γ is increased, the probability of false alarm will decrease but the probability of detection will also decrease, and vice versa. Our empirical studies indicate that the detector is relatively insensitive to the value of γ within a certain range. We have obtained good results with $\gamma = 0.01$. The spectrum envelope detector is obtained by averaging over T decision samples. A decision on whether a spectrum envelope change has occurred is made periodically once every T samples. The decision for the ℓth period is given by

$$\bar{D}_\ell = \begin{cases} 1, & \text{if } \frac{1}{T} \sum_{t=0}^{T-1} \hat{D}_{t+(\ell-1)T} > \eta, \\ 0, & \text{otherwise,} \end{cases} \tag{9}$$

for $\ell = 1, 2, \ldots$, where $\eta \in (0, 1)$ can be adjusted to provide the desired tradeoff between the false alarm and detection probabilities.

IV. Numerical Results

In this section, we describe several numerical experiments, implemented in MATLAB, that were conducted to study the performance of the proposed cepstrum-based spectrum envelope detector. We simulate phases 1 and 2 as described in Section III as follows. In phase 1, the channel state sequences for all the PUs are the same, which means that all of the PUs occupy and release the band simultaneously. Hence, when the recursive algorithm in [7] is applied, the entire band is characterized as a single PU channel. Meanwhile, in phase 2, the channel state sequences for all the PUs are generated independently such that the spectrum envelope will change over the band.

We assume that there are three PUs transmitting on three adjacent channels with the same bandwidth $\mathrm{BW} = 330$ kHz.

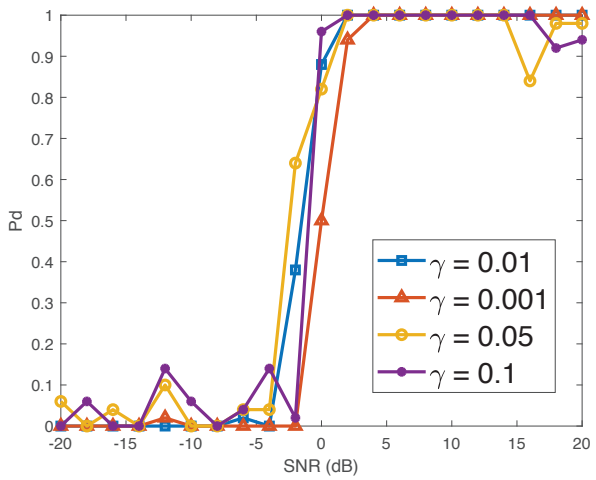

Fig. 2: Spectrum envelope detection probability vs. SNR for different values of γ ($P_{\text{fa}} = 0.01$).

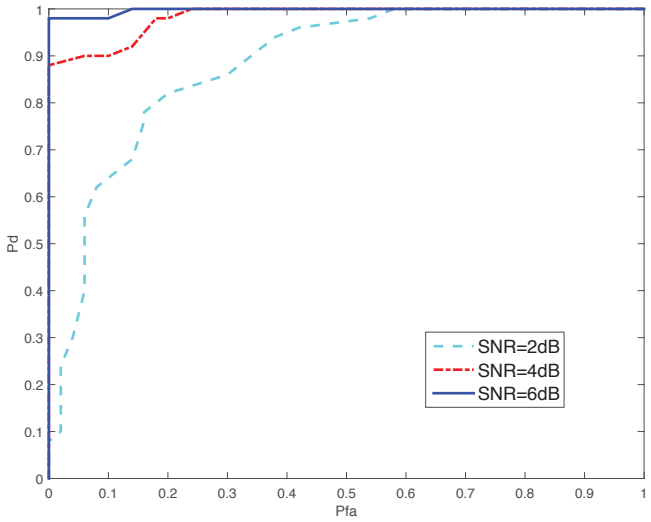

Fig. 3: ROC curves of the spectrum envelope detector under SNR values of 2, 4, and 6 dB.

The sampling rate is $F_s = 10$ MHz. The signals of both PUs are modulated by BPSK. Between each pair of adjacent channels there is a guard band with bandwidth $\text{BW}_g = 60$ kHz. To simulate the active and idle state transitions, the state sequences for both PUs are generated based on the high-order HBMM parameter ($r = 10$) estimated via the algorithm in [5] from the spectrum measurement data in [2]. For all experiments, we obtain $T_{\text{train}} = 200$ observation samples in phase 1 for parameter estimation. For performance evaluation in phase 2, the number of observation samples for each decision period for the spectrum envelope detector in (9) is set to $T = 200$ and the total number of decision periods is set to 50.

A. Signal-to-Noise Ratio

We conducted numerical experiments to explore the probability of detection under various SNR values for the cepstrum-based spectrum envelope detector. For most of the experiments, we set the HBMM parameter to $r = 1$, which simplifies the HBMM to an HMM. For cepstral feature extraction, the number of samples for calculating cepstrum is $N = 256$ and the total size of the cepstral component vector is $K = 2^{\lceil \log_2(N) \rceil}$ where $\lceil \cdot \rceil$ denotes the ceiling operator. This formula for K is used in all of our numerical experiments. The size of the cepstral feature vector $\boldsymbol{c}_w$ in (6) is set to 11, i.e., $L = 12$. We use the zeroth component, $c_w(0)$, of the cepstrum as the observation data for HBMM-based spectrum sensing since it is closely related to the energy of the signal.

Figure 2 depicts the probability of detection of the cepstrum-based spectrum envelope detection scheme for several values of γ under SNR from -20 to 20 dB when the false alarm rate is $P_{\text{fa}} = 0.01$. Evidently, the performance of the spectrum envelope detector is not very sensitive to the value of γ. The spectrum envelope detector performs well in the regime of moderate to high SNR. Taking into consideration that the SUs in the cognitive radio network transmit with low power, they will not cause harmful interference to the PUs if the SNR of a given received PU signal is quite low at their locations. Consequently, in dynamic spectrum access, the SUs generally focus their sensing efforts more on PU signals with moderate to high SNR. Figure 3 shows the receiver operating characteristic (ROC) performance of the cepstrum-based spectrum envelope detector for different SNR values of 2, 4, and 6 in units of dB. The threshold $\gamma = 0.01$ and we vary η to obtain the ROC curve. In the ROC diagram, the x-axis is the probability of false alarm P_{fa} and the y-axis is the probability of detection P_{d}. In this case, the number of samples used for cepstral feature extraction is $N = 128$. When the SNR is greater than 6 dB, almost all of the spectrum envelope changes are detected correctly.

B. Number of Samples Per Observation

We have also studied the performance impact of the number of samples N used for cepstral feature extraction. Here, the signal is generated under an SNR value of 0 dB. As before, we set $L = 12$ and $r = 1$. In Fig. 4, the performance of the proposed spectrum envelope is shown for $N = 128, 192, 256$. It turns out that the performance increases dramatically with a small increment of the number of samples N. Even when the SNR is only 0 dB, the performance is still acceptable when $N = 256$.

C. Number of Underlying States

We have compared the performance of the proposed spectrum envelope detector with different values of r, the number of states of the underlying auxiliary process S of the HBMM; in particular, we set $r = 1, 2, 5, 10$. The signal is generated under an SNR of 3 dB. The number of received signal samples used for cepstral feature extraction is $N = 128$. Figure 5 shows that the performance of the proposed spectrum envelope

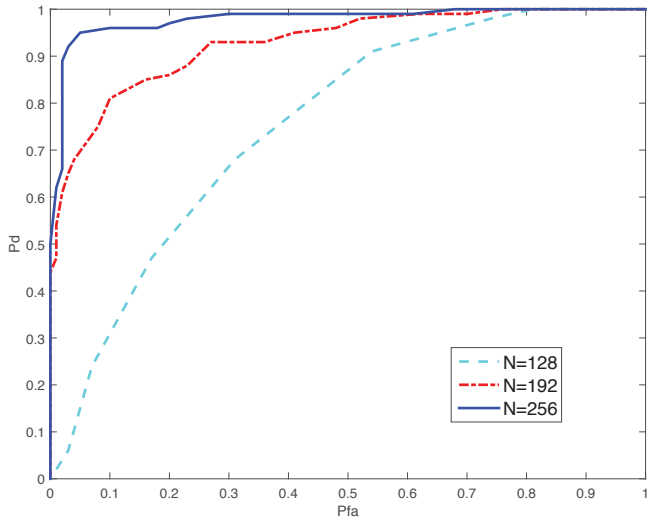

Fig. 4: ROC curves of the spectrum envelope detector with $N = 128, 192, 256$ (SNR $= 0$ dB).

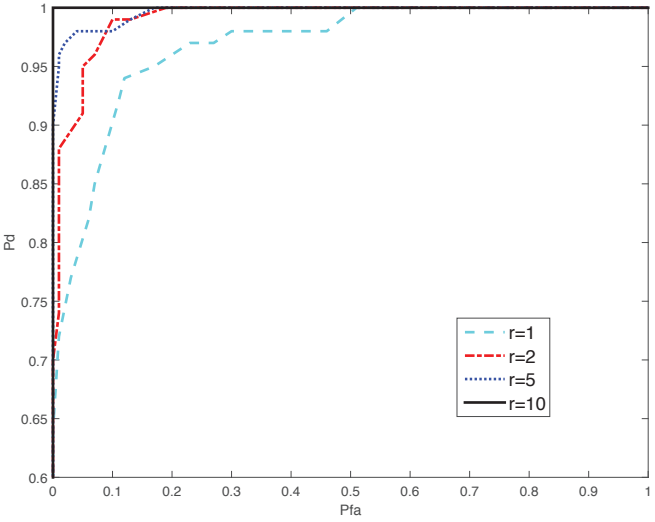

Fig. 5: ROC curves of the spectrum envelope detector with the HBMM parameter $r = 1, 2, 5, 10$ (SNR = 3 dB).

detector improves when r increases. The ROC curves of $r = 2, 5, 10$ are close to each other but are all much better than that of $r = 1$. In particular, the performance of the proposed detector is almost perfect when $r = 10$. However, $r = 2$ is more feasible in practice since the computational complexity increases exponentially as r increases while the performance is not improved much when $r > 2$.

V. Conclusion

We have proposed a cepstrum-based scheme for detecting a change in the configuration of a primary user channel in conjunction with a hidden bivariate Markov model for wideband temporal spectrum sensing. Such a change is indicated by a change in the spectrum envelope of the signal occupying the channel. The observation data for hidden Markov modeling consists of a cepstral feature vector extracted from the first several low-order cepstral components of the received signal except for the energy-dependent zeroth order component. The proposed spectrum envelope detector can be computed efficiently. Our numerical results show that the cepstrum-based spectrum envelope detector performs well in moderate to high SNR environments. In ongoing work, we are investigating the use of feature vectors based on the cyclostationary spectrum for efficiently detecting spectrum envelope changes in low SNR scenarios.

References

[1] FCC, "Spectrum policy task force," Rep. ET Docket, Federal Communications Commission, Tech. Rep. 02-135, Nov. 2002.

[2] Shared Spectrum Company, "General survey of radio frequency bands: 30 MHz to 3 GHz," Tech. Rep., August 2010. [Online]. Available: http://www.sharedspectrum.com

[3] Q. Zhao and B. M. Sadler, "A survey of dynamic spectrum access," *IEEE Signal Process. Mag.*, vol. 24, no. 3, May 2007.

[4] T. Yucek and H. Arslan, "A survey of spectrum sensing algorithms for cognitive radio applications," *IEEE Communications Surveys and Tutorials*, vol. 11, no. 1, pp. 116–130, 2009.

[5] T. Nguyen, B. L. Mark, and Y. Ephraim, "Spectrum sensing using a hidden bivariate Markov model," *IEEE Trans. Wireless Commun.*, vol. 12, no. 9, pp. 4582–4591, Sep. 2013.

[6] Y. Sun, B. L. Mark, and Y. Ephraim, "Online parameter estimation for temporal spectrum sensing," *IEEE Trans. Wireless Commun.*, vol. 14, no. 8, pp. 4105–4114, Aug. 2015.

[7] J. M. Bruno and B. L. Mark, "A recursive algorithm for wideband temporal spectrum sensing," *IEEE Trans. Commun.*, vol. 66, no. 1, pp. 26–38, Jan. 2018.

[8] Y. Sun, B. L. Mark, and Y. Ephraim, "Collaborative spectrum sensing based on hidden bivariate Markov models," *IEEE Trans. Wireless Commun.*, vol. 15, no. 8, pp. 5430–5439, Aug. 2016.

[9] J. M. Bruno, B. L. Mark, Y. Ephraim, and C.-H. Chen, "A computing budget allocation approach to multiband spectrum sensing," in *IEEE Wireless Comm, and Networking Conf. (WCNC)*, Mar. 2017.

[10] R. B. Randall, "A history of cepstrum analysis and its application to mechanical problems," *Mechanical Systems and Signal Processing*, vol. 97, pp. 3–9, Dec. 2016.

[11] R. H. Shumway, D. R. Baumgardt, and Z. A. Der, "A cepstral F statistic for detecting delay-fired seismic signals," *Technometrics*, vol. 40, no. 2, pp. 100–110, May 1998.

[12] Y. Ephraim and M. Rahim, "On second-order statistics and linear estimation of cepstral coefficients," *IEEE Trans. Speech Audio Process.*, vol. 7, no. 2, pp. 162–176, Apr. 1999.